

UNCERTAINTY ESTIMATION IN COMPLEX PERMITTIVITY MEASUREMENTS BY SHIELDED DIELECTRIC RESONATOR TECHNIQUE USING THE MONTE CARLO METHOD

E. Páez¹, M. A. Azpúrua^{1, *}, C. Tremola¹, and R. C. Callarotti²

¹Instituto de Ingeniería, Laboratorio de Electromagnetismo Aplicado, Centro de Ingeniería Eléctrica y Sistemas, Caracas, Venezuela

²Instituto Venezolano de Investigaciones Científicas (IVIC), Caracas, Venezuela and Universidad del Turabo, Gurabo, Puerto Rico

Abstract—In this paper, we estimate the uncertainty in complex permittivity measurements performed in a shielded dielectric resonator, by using the Monte Carlo Method. We selected this approach since the theoretical expressions required to interpret the experimental results are highly non-linear. Furthermore the resonant frequency of the system and its quality factor are highly correlated. Thus we propose a model for the measurement process which considers the major sources of uncertainty previously reported in published experimental results. The proposed model combined with the Monte Carlo method was used to propagate the probability distributions of each uncertainty contribution, obtaining a) the approximate probability density function for the measured complex permittivity, and b) the estimated expanded uncertainty for the mode TE₀₁₁. The results show that this procedure leads to small uncertainty intervals for the real part of the dielectric permittivity, while it is not very reliable in the loss tangent measurement. Additionally, for each input quantity, we calculated the standard deviation in the experimental results produced independently by each uncertainty contribution.

1. INTRODUCTION

Resonance methods represent one of the most useful techniques for the measurement of the complex permittivity of low-loss materials [1–3], offering the highest possible accuracy in measurements of real

Received 13 April 2012, Accepted 15 May 2012, Scheduled 29 May 2012

* Corresponding author: Marco A. Azpúrua (bazpuru@fii.gob.ve).

permittivity [4–6]. Resonant cavities having axial symmetry are the most commonly used resonators in dielectric metrology. In the present work we chose a cylindrical resonator since the relationship between sample dielectric permittivity, cavity dimensions, resonant frequency and unloaded Q factor, can all be derived theoretically by separation of variables [5–8].

Since measurement uncertainties will affect the experimental results, the accuracy of the complex permittivity measurements can only be estimated once the uncertainty sources are identified and their effect modeled as part of the measurement process.

Some uncertainty sources are associated to geometrical factors such as resonator size and sample shape and dimensions. Their effect can be reduced by careful size measurements and careful construction of the resonators. One fundamental measurement limitation is due to the inherent measurement accuracy of the Vector Network Analyzer (VNA). Also, the sensitivity of the measurement system respect to the input variables must be understood in order to determine the conditions under which a given method may be used effectively in electromagnetic measurement characterization [9, 10].

Thus, the estimation of the uncertainty associated to complex permittivity measurements is a challenging task, previously addressed using a simplified approach [10] that assumed that all the contributions are uncorrelated and symmetric, combining them in a linear or linearized model using the error propagation law within the framework of the Guide to the expression of Uncertainty in Measurement, GUM [11]. Since those assumptions may affect the reliability of the results, it is advisable to use alternative methods, such as Monte Carlo Method, for the calculation and validation of measurement uncertainty [12].

The Monte Carlo Method (MCM) is recognized as a practical alternative by the Joint Committee for Guides in Metrology (JCGM) of the Bureau International des Poids et Mesures (BIPM), and it has been included in the GUM as a supplement, since 2008 [12]. It has been widely used within many scientific disciplines, such as metrology, geodesy, optics, hydrology, electronics, structural mechanics and electromagnetic compatibility, among others [13–19].

The paper is organized as follows: in Section 2 we describe the foundations and the general methodology used for the measurement of complex permittivity in shielded dielectric resonators. In Section 3 we describe measurement uncertainties using the MCM approach in the context of GUM. In Section 4 we propose a model for the measurement process and discuss the different uncertainty contributions. In Section 5, we present a numerical example based on our measurement

system that will illustrate the methodology discussed. Finally, we conclude by discussing the probability distribution of the results and the confidence intervals achieved in the numerical examples.

2. COMPLEX PERMITTIVITY MEASUREMENTS BY SHIELDED DIELECTRIC RESONATOR TECHNIQUE

For a specific mode excited in the resonant structure containing the sample, the measured basic variables are the resonant frequency and Q -factor for that mode. The complex permittivity of the sample can be evaluated from these two measured quantities, provided all other parameters of the structure (dimensions and the surface resistance of the metallic enclosure) are known [5, 7].

Exact relations among permittivity, sample and cavity dimensions, measured resonant frequency and the unloaded Q -factor can only be derived if we can carry out an accurate theoretical analysis for the resonant structures. Theoretical results (obtained by separation of variables) can be derived in the case of the shielded dielectric resonator with cylindrical symmetry, which was selected for our analysis and measurements. We additionally assume that all metal parts are made of perfect conductors (infinite conductivity).

Figure 1 shows the case of a cylindrical dielectric resonator enclosed by a metal shield, where b is the cavity resonator radius, a is the dielectric rod radius and d is the height of the cavity. This type of cavity resonator can be analyzed as a cylindrical waveguide enclosing a central sample of radius a , and terminated in perfectly conducting plates.

The electromagnetic fields, for TE_{mnp} modes, in both the dielectric rod and the rest of the inner volume of the cavity resonator can be determined using the theory of Hertzian potentials [7]. In the structure, the magnetic Hertzian potential, Π_m , in the cylindrical

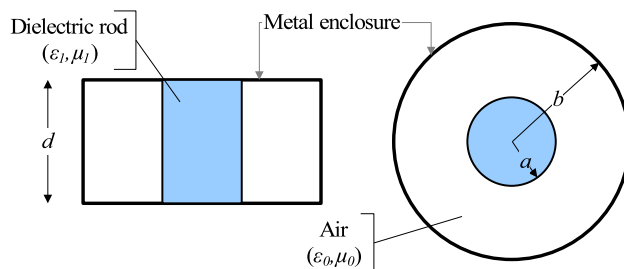


Figure 1. Cylindrical shielded dielectric resonator.

coordinate system, is given by [7, 20],

$$\mathbf{\Pi}_m(\rho, \varphi, z) = [J_n(k_c\rho) + Y_n(k_c\rho)] \cos(n\phi) \sin(\beta z) \hat{\mathbf{a}}_z, \quad (1)$$

where, $J_n(k_c\rho)$ is the Bessel function of the first kind evaluated in $k_c\rho$, $Y_n(k_c\rho)$ the Bessel function of the second kind evaluated in $k_c\rho$, k_c the cutoff wavenumber, and β is given by,

$$\beta = \frac{p\pi}{d}, \quad (2)$$

The electric \mathbf{E} field and the magnetic \mathbf{H} field are calculated using,

$$\mathbf{E} = -j\omega\mu\nabla \times \mathbf{\Pi}_m, \quad (3)$$

$$\mathbf{H} = \nabla \times \nabla \times \mathbf{\Pi}_m. \quad (4)$$

It is important to note that the magnetic Hertzian potential (1) is valid for both regions of the shielded resonator, with the clear understanding that in the dielectric rod ($0 \leq \rho \leq a$) only the Bessel function of the first kind is allowed as part of the solution since $Y_n(k_c\rho)$ goes to infinity at the origin.

Then, the boundary conditions of the tangential electric field at $\rho = b$ and $\rho = a$ and the continuity of the tangential magnetic field at $\rho = b$ provide the relationship between the resonance frequency of the loaded cavity resonator and the relative dielectric permittivity of the measured sample, given by [21],

$$\frac{nk_{c0}^2\mu_1}{ak_{c1}^2\mu_0} - \frac{k_{c0}^2\mu_1}{k_{c1}\mu_0} \frac{J_{n+1}(k_{c1}a)}{J_n(k_{c1}a)} = \frac{n\alpha}{a} - k_{c0} \frac{\alpha J_{n+1}(k_{c0}a) + Y_{n+1}(k_{c0}a)}{\alpha J_n(k_{c0}a) + Y_n(k_{c0}a)}, \quad (5)$$

where,

$$\alpha = -\frac{nY_n(k_{c0}b) - bk_{c0}Y_{n+1}(k_{c0}b)}{nJ_n(k_{c0}b) - bk_{c0}J_{n+1}(k_{c0}b)}, \quad (6)$$

and,

$$\frac{k_{c1}^2 + \beta^2}{k_{c0}^2 + \beta^2} = \frac{\mu_1\varepsilon_1}{\mu_0\varepsilon_0}, \quad (7)$$

where the cutoff wavenumber of both media (the unknown dielectric k_{c1} and the air k_{c0}) is related to the angular resonance frequency, $\omega = 2\pi f$, as follows,

$$k_{c1}^2 = \omega^2\mu_1\varepsilon_1 - \beta^2, \quad (8)$$

$$k_{c0}^2 = \omega^2\mu_0\varepsilon_0 - \beta^2. \quad (9)$$

The only parameter that must be measured in order to calculate the real part of the dielectric permittivity is the resonance frequency, f . Hence, Equations (5) and (7) are numerically evaluated and solved to obtain the real part of the dielectric permittivity of the unknown

dielectric medium. Nevertheless, (6) and (7) can be simplified for the particular case of TE₀₁₁, as shown in, (10) and (11) [6, 7],

$$\frac{k_{c0}\mu_1 J_1(k_{c1}a)}{k_{c1}\mu_0 J_0(k_{c1}a)} = \frac{\alpha J_1(k_{c0}a) + Y_1(k_{c0}a)}{\alpha J_0(k_{c0}a) + Y_0(k_{c0}a)}, \quad (10)$$

$$\alpha = -\frac{Y_1(k_{c0}b)}{J_1(k_{c0}b)}. \quad (11)$$

On the other hand, if the unknown medium has dielectric losses ($\varepsilon_1 = \varepsilon'_1 - j\varepsilon''_1$), it will be necessary to measure the system quality factor [4], Q , and the loss tangent, $\tan(\delta_d)$, both given by,

$$\frac{1}{Q} = \frac{1}{Q_d} + \frac{1}{Q_u} = \frac{\Delta f}{f} = \frac{f_u - f_l}{f}, \quad (12)$$

$$\tan(\delta_d) = \frac{1}{Q_d} = \frac{\varepsilon''_1}{\varepsilon'_1}, \quad (13)$$

where f is the resonant frequency, Δf the bandwidth of 3 dB, f_l the lower frequency of Δf , f_u the upper frequency of Δf , Q_d the quality factor associated only to dielectric losses, and Q_u the quality factor of the unloaded cavity associated with the finite conductivity of the metal enclosure, which is given by,

$$Q_u = \frac{\omega W}{P_c}, \quad (14)$$

where W is the total stored energy inside the empty cavity and P_c the power loss in the conducting walls. For a given TE_{*nmp*} mode in an unloaded cylindrical cavity, Q_u can be calculated using the following relation [21],

$$Q_u = \frac{(kb)^3 \eta_0 bd}{4(p'_{nm})^2 R_s} \frac{1 - \left(\frac{n}{p'_{nm}}\right)^2}{\left\{ \frac{bd}{2} \left[1 + \left(\frac{\beta bn}{(p'_{nm})^2}\right)^2 \right] + \left(\frac{\beta b^2}{p'_{nm}}\right)^2 \left[1 - \left(\frac{n}{p'_{nm}}\right)^2 \right] \right\}}, \quad (15)$$

where k and η_0 are the wavenumber and impedance of free space, p'_{nm} the m -th root of the first derivative of the Bessel function of the first kind, and R_s the surface resistance of the walls:

$$R_s = \sqrt{\frac{\omega\mu_0}{2\sigma}}. \quad (16)$$

3. UNCERTAINTY ESTIMATION USING MONTE CARLO METHOD

In general, the functional relationship (i.e., measurement model or equation) between the measurand (quantity intended for measurement)

Y and the set of input quantities $\{X_1, X_2, \dots, X_N\}$ determined in a measurement process is given by,

$$Y = f(X_1, X_2, \dots, X_N). \quad (17)$$

The measurement model f includes both corrections for systematic effects and accounts for sources of variability, such as those due to different observers, instruments, samples, laboratories and times at which observations are made. Therefore, the general functional relationship describes a physical law but also describes a measurement process. Some of the variables involved in the general functional relation can be controlled directly or indirectly, others can be observed but not controlled and some cannot even be observed.

An estimate of the measurand Y , denoted by y , is obtained from (17) using input estimates $\{x_1, x_2, \dots, x_N\}$ for the values of the N quantities $\{X_1, X_2, \dots, X_N\}$. Thus the output estimate y , which is the result of the measurement, is given by,

$$y = f(x_1, x_2, \dots, x_N). \quad (18)$$

The estimated standard deviation associated with the output estimate or measurement result y , is defined as the combined standard uncertainty and denoted by $u_c(y)$. It is determined from the estimated standard deviation associated with each input estimate x_i , defined as the standard uncertainty and denoted by $u(x_i)$ [11].

Each input estimate x_i and its associated standard uncertainty $u(x_i)$ are obtained from a distribution of possible values of the input quantity X_i . This probability distribution may be experimentally determined, that is, based on a series of observations $X_{i,j}$ of X_i , (determined experimentally) or it may be a distribution defined a priori. Type A evaluations of standard uncertainty components are founded on frequency distributions while Type B evaluations are founded on a-priori distributions [11]. In both cases it must be recognized that the probability distributions are models that are used to represent the state of our knowledge [11] about the sources of uncertainty.

In Monte Carlo techniques, both, the random and the systematic components of the uncertainty, are treated as having a random nature. It is important to notice that the systematic component is not modeled as random, and it is the knowledge about the systematic component for which a probability distribution is introduced [12].

This method basically involves randomly generating a number M of Monte Carlo trials (i.e., the number of model evaluations made) where the distribution function of the output quantity, Y , will be numerically approximated. It is further assumed that the

probability densities of the considered input quantities are known a priori. Then, a sample vector of the input quantities can be drawn repeatedly using pseudo random number generators. For each input sample vector, the corresponding values of the output quantities are calculated by using the corresponding functional relation. The set of output sample vectors yields an empirical distribution which can be used to approximate the distribution of the output quantities. All required measures (expectation value, variance and covariance) as well as higher-order central moments such as skewness and kurtosis can then be derived [14]. Before applying MCM, the conditions for valid application should be verified [12]. It is recommended to use $M \geq 10^6$ to estimate a 95% coverage interval for the output quantity to ensure such that this length is correct to one or two significant decimal digits [12]. It is also recommended to validate the quality of the pseudo-random number generator to be used in the calculations [12].

The MCM is implemented using an algorithm that can be summarized as follows [13]:

- (i) There must be generated a set of N input parameters $\{x_1, x_2, \dots, x_N\}$, which are random variables distributed according to a probability density function assigned to each input parameter. This process should be repeated M times.
- (ii) The functional relationship that model the measurement system is then evaluated to obtain the output,

$$y_j = f(x_{1,j}, x_{2,j}, \dots, x_{N,j}), \quad (19)$$

for $j = 1, 2, \dots, M$. From this sample, it is possible to estimate the probability density function of y .

- (iii) The relevant estimates of any statistical quantity can then be calculated (average, variance, skewness and kurtosis of the output, among others).
- (iv) The output vector $\{y_1, y_2, \dots, y_N\}$ is sorted in ascending order to obtain a vector $\tilde{y} = \{\tilde{y}_1, \tilde{y}_2, \dots, \tilde{y}_N\}$.
- (v) The confidence interval $[\tilde{y}_r, \tilde{y}_s]$ is found approximately through the components of \tilde{y} identified by the indexes given by (20) and (21) [22]:

$$r = \text{round}((M + 1)\gamma), \quad (20)$$

$$s = \text{round}((M + 1)(1 - \gamma)), \quad (21)$$

where, γ is the significance level ($\gamma = 0.025$ for 95% of confidence) and the function $\text{round}(x)$ is used to represent the nearest integer to x .

4. THE MEASUREMENT PROCESS

The measurement methodology is the following: Q_u and f are measured first with the empty resonator cavity and then with the dielectric rod in place. The measurements are made with a VNA. This information is used in (5) and (7) to numerically calculate the relative dielectric permittivity and in (12) and (13) to calculate the loss tangent. However, the measurement results are reliable only if within the measurement process is provided that [5]:

- The unloaded cavity losses are very low, that is, $15000 \leq Q_u \leq 30000$.
- The sample is homogeneous and has no magnetic losses. Therefore, the sample should be carefully selected and well prepared.
- The dielectric losses do not affect significantly the resonance frequency, that is, $\tan(\delta_d) \leq 0.1$.

Finally, it is important to notice that this kind of cavities can be excited by different modes. The selection of the operation mode must take into account the type of measurement required (permittivity or permeability) so as to select the most appropriate magnetic or electric field geometry for the optimal interaction with the sample.

In practice, it is recommended to choose one of the few first modes of the frequency spectrum, so that the measurements will be less sensitive to geometrical imperfections. Finally, the mode selected should correspond to a simple pattern distribution so as to allow easier identification. In our case these were the reasons for the selection of the mode TE_{011} for the measurement of permittivity.

Taking into account the previous considerations, we now proceed to identify the significant sources of uncertainty that will contribute to the overall uncertainty of the experimental results.

4.1. Sources of Uncertainty

The variables needed for the determination of the dielectric permittivity are affected mainly by the following uncertainty contributions: a) the accuracy of the instruments used in the measurements, b) the influence of the resolution of the measuring instrument and c) the repeatability of the results. In each Monte Carlo iteration, the combination of all the mentioned uncertainty factors associated to the nominal specifications is treated as a measurement error. A summary of the sources of uncertainty in complex permittivity measurements by shielded dielectric resonator technique is shown in Table 1.

Table 1. Sources of uncertainty in complex permittivity measurements by shielded dielectric resonator technique.

Factor	Error	Source of Uncertainty	Type of evaluation	Probability Distribution	Parameters
<i>d</i>	<i>e_d</i>	Accuracy	B	Uniform	MAE
		Resolution	B	Triangular	SD
		Repeatability	A	Normal	<i>s₀</i>
<i>a</i>	<i>e_a</i>	Accuracy	B	Uniform	MAE
		Resolution	B	Triangular	SD
		Repeatability	A	Normal	<i>s_o</i>
<i>b</i>	<i>e_b</i>	Accuracy	B	Uniform	MAE
		Resolution	B	Triangular	SD
		Repeatability	A	Normal	<i>s_o</i>
<i>f</i>	<i>e_f</i>	Calibration	B	Normal	<i>U_{cal}</i>
		Resolution	B	Uniform	SF

The errors associated with the dimensional factors, *e_d*, *e_a* and *e_b*, are given by the sum of the error related to the accuracy of the measurement instrument, *e_α*, the error related to the resolution of the measurement instrument, *e_r*, and other errors that affects the repeatability, *e_o*. The uncertainties contributions due to *e_α* and *e_r* are defined in terms of the maximum allowable error (MAE), and the scale division (SD), respectively. Hence, the probability density functions of *e_α*, *f* (*e_α*) and *e_r*, *f* (*e_r*), are given by,

$$f(e_\alpha) = \begin{cases} \frac{1}{\text{MAE}} & \text{for } -\frac{\text{MAE}}{2} \leq e_\alpha \leq \frac{\text{MAE}}{2} \\ 0 & \text{for } e_\alpha < -\frac{\text{MAE}}{2} \text{ or } e_\alpha > \frac{\text{MAE}}{2} \end{cases} \quad (22)$$

and,

$$f(e_r) = \begin{cases} \frac{4}{\text{SD}^2}e_r + \frac{2}{\text{SD}} & \text{for } 0 \leq e_r \leq \frac{\text{SD}}{2} \\ -\frac{4}{\text{SD}^2}e_r + \frac{2}{\text{SD}} & \text{for } -\frac{\text{SD}}{2} \leq e_r < 0 \\ 0 & \text{for } e_r < -\frac{\text{SD}}{2} \text{ or } e_r > \frac{\text{SD}}{2} \end{cases} \quad (23)$$

The variable *e_o* is modeled as a random variable with normal distribution, zero mean and an estimated standard deviation, *s_o*, where *s_o* is calculated through the repeated measurement of the length of *d*, *a*, and *b*.

On the other hand, e_f is obtained as the sum of the error related to the accuracy of the calibration of the VNA, e_{cal} , and the error due to rounding the value of the frequency measured in units of gigahertz to the third significant figure, e_{SF} . e_{cal} is modeled as an unbiased random variable of normal distribution with a standard deviation equal to σ_{cal} , where σ_{cal} (standard uncertainty) is obtained from the calibration certificate of the VNA as the expanded uncertainty reported, U_{cal} , divided by the coverage factor, k (usually $k = 2$ for a 95% of confidence level). In the same way, e_{SF} is modeled as an unbiased uniformly distributed random variable taking values within $-500 \text{ kHz} \leq e_{SF} \leq 500 \text{ kHz}$. In order to reduce the influence of the repeatability of the frequency measurements as an uncertainty contribution, it is recommended to configure the VNA to perform the averaging of the readings automatically.

Additionally, the effect of the air gap between the dielectric rod and the cavity bottom is not a source of uncertainty because the circumferential electric field distribution that characterizes the TE_{01n} modes [5] allows the air gap to be omitted without affecting the measurement. Another minor effect is related to the possible lack of alignment between the vertical axis of the dielectric rod with respect to the vertical axis of the metallic cylinder. Previous simulations, using a finite element solver, revealed that this source of uncertainty is not significant (provided that this misalignment is less than a millimeter) since the error involved is smaller than the numerical errors incurred in computing.

Finally, other factors that might contribute to the uncertainty in complex permittivity measurements, such as sample properties heterogeneities and eccentricity of the cavity walls, are not considered, assuming that the sample under test is well prepared and that the cavity has been carefully constructed.

4.2. A Model of the Measurement Process

In order to estimate the uncertainty in the complex permittivity measurements obtained by shielded dielectric resonator technique, we begin by analyzing the measurement process according to the formulation discussed in Section 2. Starting from a set of nominal specifications such as the characteristics of a given dielectric for the sample under test, cavity dimensions (designed to resonate approximately at a desired frequency for the selected mode), and conductivity of the metal enclosure; the nominal direct measurement results are calculated theoretically, as shown in Figure 2.

The random errors associated with the uncertainty contributions of each influencing factor are added to the nominal specifications

in order to calculate the new direct measurement results (f_m , f_{um} and f_{lm}) and consequently the indirect measurement results ϵ'_{1m} and $\tan(\delta_d)$ are random variables of unknown Probability Density Function (PDF). The errors are generated using the pseudo-random number generators included in MATLABTM, because they meet the requirements of the Monte Carlo Method as mentioned in Section 3. Figures 3 and 4 show the relationships between the errors in the measurement process.

It is important to notice that the cavity resonant frequency depends on the variations in the dimensions of the cavity with respect to the nominal ones. The measured resonance frequency is also affected by the measurement errors of the VNA. This situation affects the experimental results, ϵ'_{1m} and $\tan(\delta_{dm})$, in a way that can only be evaluated after a great number of iterations.

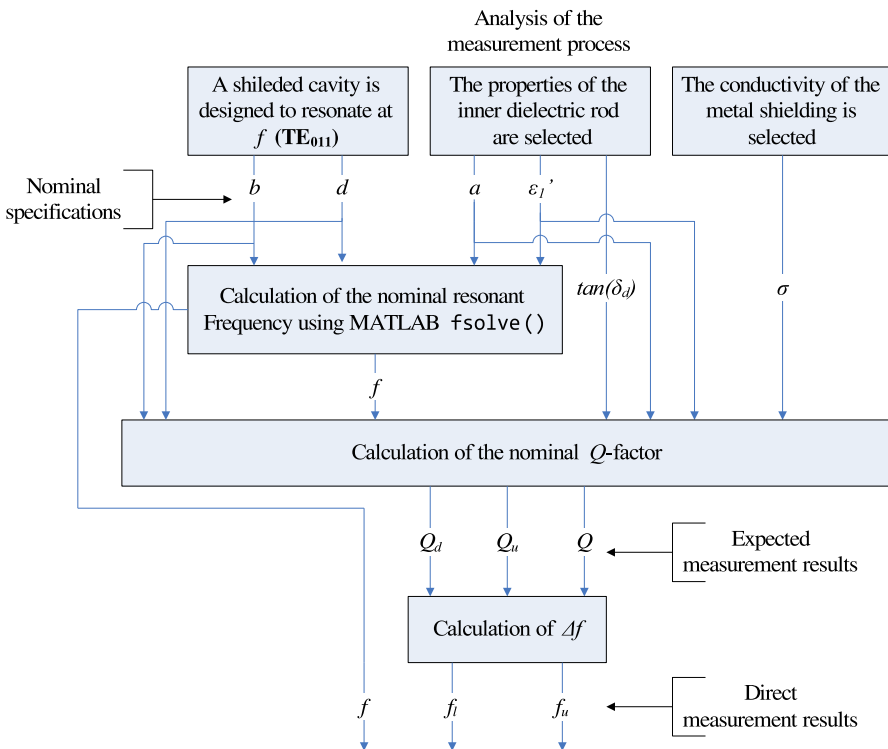


Figure 2. Analysis of the measurement process.

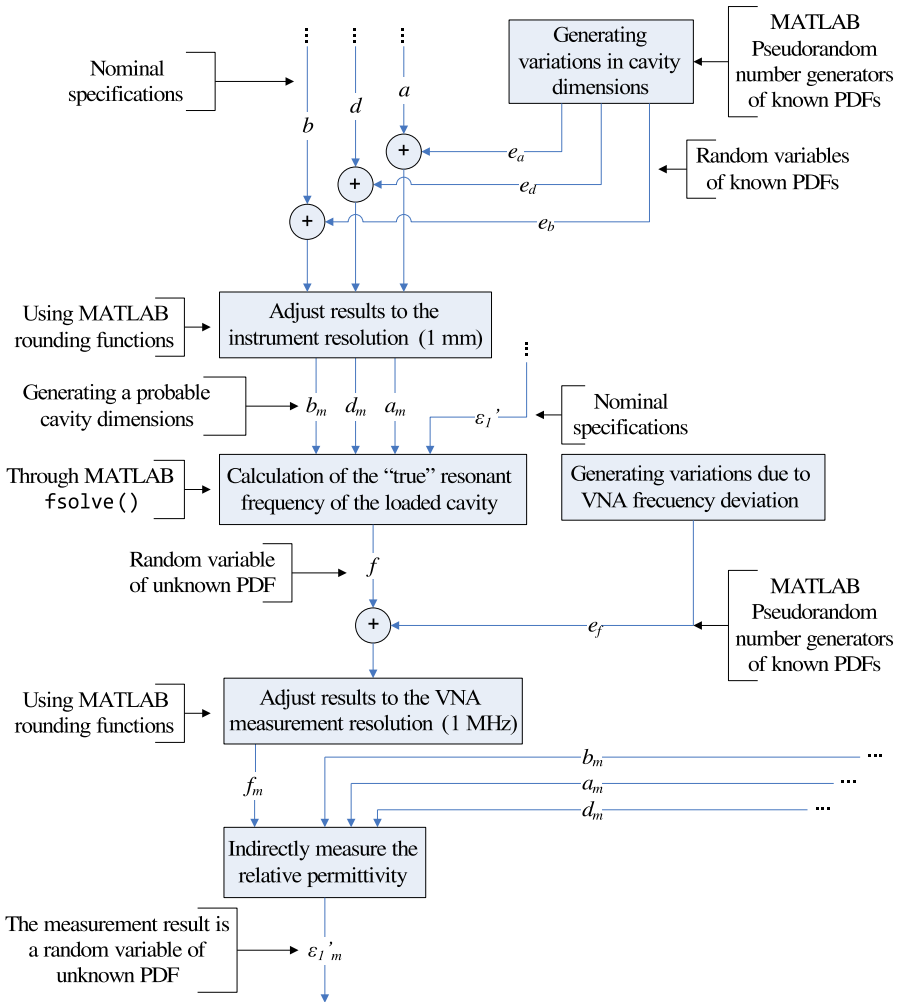


Figure 3. The model of measurement process of ϵ'_{1m} .

5. RESULTS

Now, let us consider a TE_{011} mode of a shielded resonator cavity with nominal dimensions given by $a = 14.24$ cm, $d = 7.02$ cm, used to measure the complex permittivity of an hypothetic dielectric material (similar to teflon) of $b = 3$ cm, characterized by $\epsilon'_1 = 2$ and $\tan(\delta_d) = 15 \times 10^{-4}$ at 2.5 GHz. The cavity metal enclosure is made of copper with a nominal conductivity $\sigma = 5.813 \times 10^7$ S. The nominal resonant

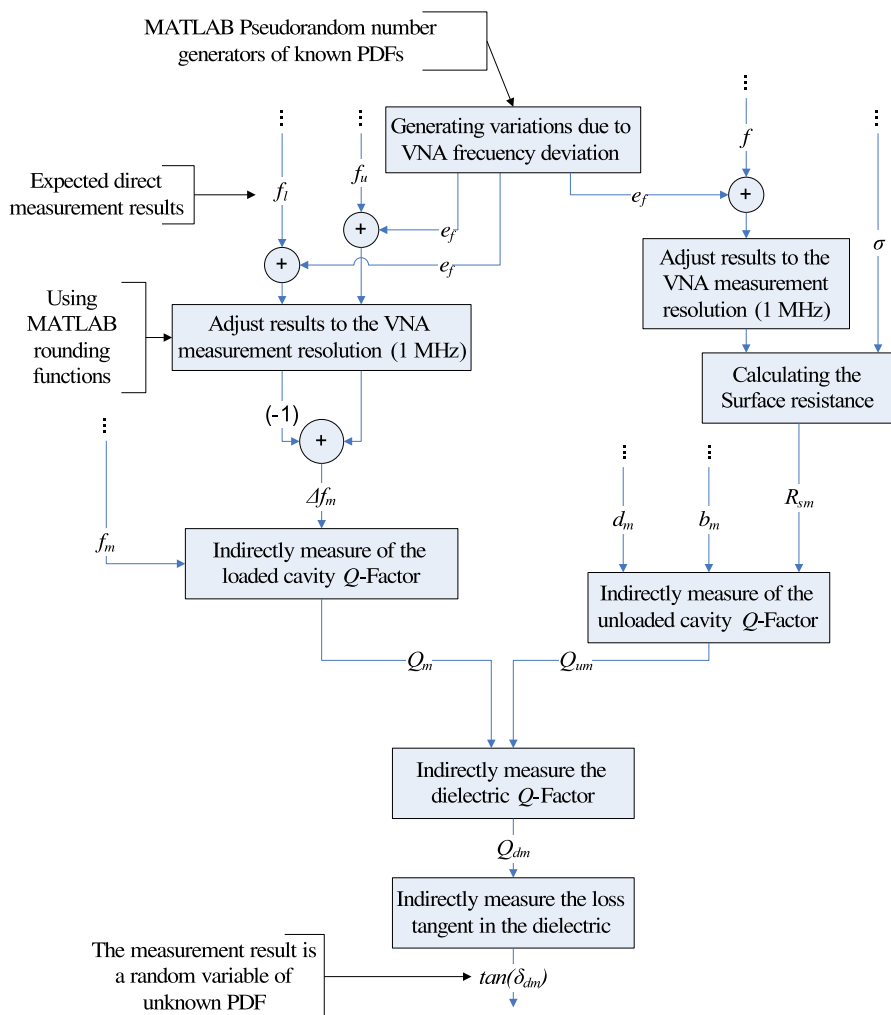


Figure 4. The model of measurement process of $\tan(\delta_{dm})$.

frequency of the empty cavity is 2.5 GHz.

Table 2 summarizes the parameters that define the PDF of the sources of uncertainty considered in this numerical example.

In the presence of the dielectric rod, the resonant frequency usually decreases. This frequency displacement could represent an important deviation of the previously calculated cavity losses, included indirectly in the system quality factor, introducing a higher uncertainty in the determination of the dielectric loss tangent. However, for our example,

the resonant frequency of the TE_{011} mode moves close to 2.45 GHz representing a low deviation. For this reason, the accuracy of resonant methods are related to materials with low loss.

The model presented in the previous section was run for 10^6 Monte Carlo trials. Figures 5 and 6 show the absolute frequency histograms of the measured relative dielectric permittivity and loss tangent, respectively.

The approximated PDF of ε'_{1m} shows a quasi-symmetrical behavior around its nominal value while $\tan(\delta_{dm})$ exhibits a highly asymmetrical distribution around its nominal value. As expected, both output distributions are not normal. This behavior corresponds mainly to the nonlinearity of (15) with variations of the cavity dimensions above and below than the nominal dimensions and the corresponding frequency shifts near 2.5 GHz. The total uncertainty in the measurement of the loss tangent becomes higher with the increasing of the conductivity losses in the cavity walls.

The 95% confidence bound related to the real part of the dielectric permittivity is $[1.9849, 2.0139]$ that is, $2^{+0.7\%}_{-0.76\%}$, and for the loss tangent is $[11.31 \times 10^{-4}, 20.84 \times 10^{-4}]$ that is, $(15 \times 10^{-4})^{+24.6\%}_{-38.9\%}$. These results show that the relative uncertainty in the determination of the loss tangent is much greater than relative uncertainty in the measurement of the dielectric permittivity.

Table 2. Values of all sources of uncertainty.

Factor	Error	Source	Parameter Value
d	e_d	e_α	MAE = 1 mm
		e_r	SD = 1 mm
		e_o	$s_o = 1$ mm
a	e_a	e_α	MAE = 1 mm
		e_r	SD = 1 mm
		e_o	$s_o = 1$ mm
b	e_b	e_α	MAE = 1 mm
		e_r	SD = 1 mm
		e_o	$s_o = 1$ mm
f	e_f	e_{cal}	$U_{cal} = 8$ kHz
		e_{SF}	SF = 1 MHz

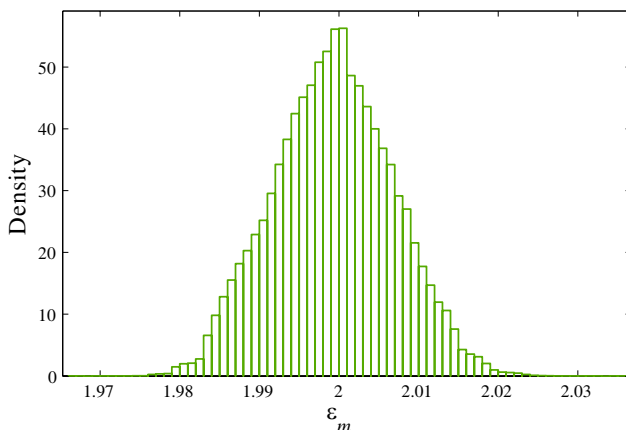


Figure 5. Frequency histograms of the measured relative dielectric permittivity.

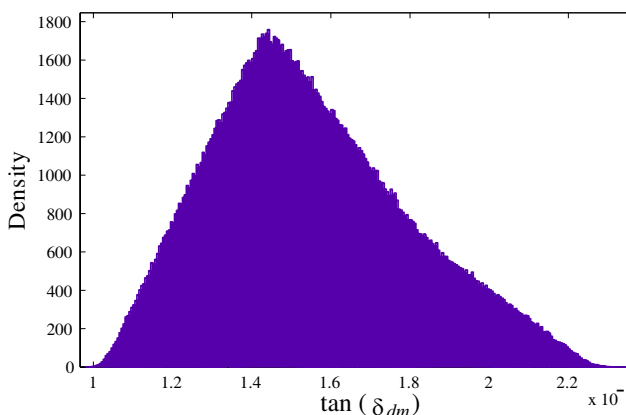


Figure 6. Frequency histograms of the measured loss tangent.

5.1. Contribution of Each Input Quantity

In order to determine which variable contributes the most to the total uncertainty in the results, the standard deviations in the results (s_ϵ and $s_{\tan(\delta)}$) were calculated running the MCM independently for each input magnitude, a , b , d and f . The results are shown in Figures 7 and 8 for the dielectric permittivity and for the loss tangent, respectively.

Figures 7 and 8 show that all input variables, approximately contribute equally to the total variability, denoted by the bar t . This means that special care should be taken on the overall measurement process.

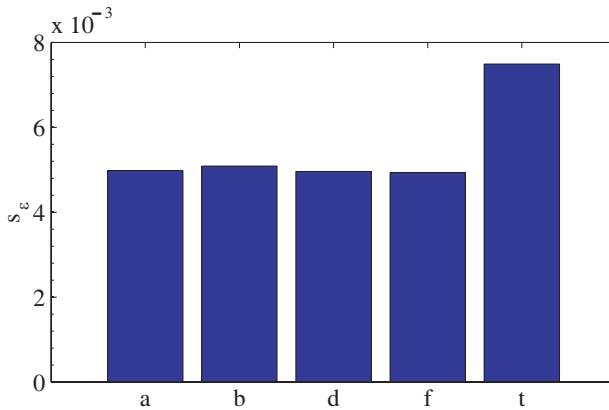


Figure 7. Contribution of each input quantity to the variability of ε'_{1m} .

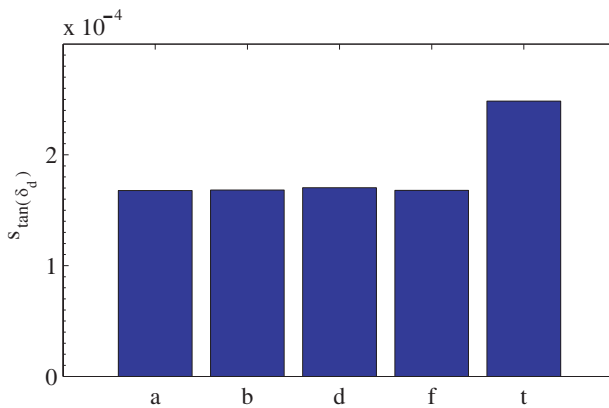


Figure 8. Contribution of each input quantity to the variability of $\tan(\delta_{dm})$.

6. CONCLUSIONS

We have shown the suitability of the Monte Carlo method in the estimation of the uncertainty associated to the complex permittivity measurements using a dielectric resonator technique inside a metallic cylindrical cavity. This procedure could also be adapted to any systems where the behavior of the electromagnetic field is known through exact equations, provided that the significant sources of uncertainty can be identified and included in the measurement model. It is important to point out that a sufficient number of runs of the Monte Carlo algorithm

should be performed in order to estimate with sufficient accuracy the uncertainty intervals of the dielectric permittivity and the loss tangent for a given confidence level.

The results presented in this paper show the advantages and disadvantages of these kinds of methods in electromagnetic characterization of materials where the experimental results for the real part of the dielectric permittivity are robust and stable while the measurement results of the loss tangent are very sensitive to the input errors. The confidence bound for the dielectric constant was approximately 1.5% wide while the loss tangent was about 65% wide, thus proving the previous statement.

We also notice that the conventional GUM analysis would not be adequate in the estimation of the uncertainty in the measurement results because the results are not normally distributed and are not symmetrical, thus justifying the Monte Carlo approach as a valid method in the uncertainty estimation. The distribution of the results attached to the sources of uncertainty identified in the measurement system used here might not be valid if other system configuration or measurement methods are use. This would be the case for transmission/reflexion methods.

Another important result, which MCM has revealed, is the sensibility of the measurement system to each input source variations. The example discussed in this paper shows that the final uncertainty is equally sensitive to all input variables, suggesting that special care must be taken in the overall process. Nevertheless, this kind of analysis is very useful in order to establish which contribution most affects the uncertainty of measurements.

REFERENCES

1. Kukharchik, P. D., V. M. Serdyuk, and J. A. Titovitsky, "Diffraction of hybrid modes in a cylindrical cavity resonator by a transverse circular slot with a plane anisotropic dielectric layer," *Progress In Electromagnetics Research B*, Vol. 3, 73–94 2008.
2. Wang, J., S. Qu, H. Ma, J. Hu, Y. Yang, and X. Wu, "A dielectric resonator-based route to left-handed metamaterials," *Progress In Electromagnetics Research B*, Vol. 13, 133–150, 2009.
3. Zhou, Y., E. Li, G. Guo, Y. Gao, and T. Yang, "Broadband complex permittivity measurement of low loss materials over large temperature ranges by stripline resonator cavity using segmentation calculation method," *Progress In Electromagnetics Research B*, Vol. 113, 143–160, 2011.

4. Chen, L. F., C. K. Ong, C. P. Neo, V. V. Varadan, and V. K. Varadan, *Microwave Electronics Measurement and Materials Characterization*, John Wiley & Sons, 2004.
5. Krupka, J., “Frequency domain complex permittivity measurements at microwave frequencies,” *Measurement Science and Technology*, Vol. 17, 55–70, 2006.
6. Yeh, Y.-S., J.-T. Lue, and Z.-R. Zheng, “Measurement of the dielectric constant of metallic nanoparticles embedded in a paraffin rod at microwave frequencies,” *IEEE Transaction on Microwave Theory and Techniques*, Vol. 53. No. 5, 2005.
7. Collin, R. E., “Field theory of guided waves,” *IEEE Antennas and Propagation Society*, 1960.
8. Liu, J., C. Chen, H. Lue, and J. Lue, “A new method developed in measuring the dielectric constants of metallic nanoparticles by a microwave double-cavity dielectric resonator,” *IEEE Microwave and Wireless Components Letters*, Vol. 13, 181–183, 2003.
9. Dester, G. D., E. J. Rothwell, M. J. Havrilla, and M. W. Hyde, “Error analysis of a two-layer method for the electromagnetic characterization of conductor-backed absorbing material using an open-ended waveguide probe,” *Progress In Electromagnetics Research B*, Vol. 26, 1–21, 2010.
10. Krupka, J., A. P. Gregory, O. C. Rochard, R. N. Clarke, B. Riddle, and J. Baker-Jarvis, “Uncertainty of complex permittivity measurements by split-post dielectric resonator technique,” *Journal of the European Ceramic Society*, Vol. 21, 2673–2676, 2001.
11. Joint Committee for Guides in Metrology, *Evaluation of Measurement Data Guide to the Expression of Uncertainty in Measurement*, 1st Edition, BIPM, Sèvres-France, 2008, Available at: <http://www.bipm.org/en/publications/guides/gum.html>, <http://www.bipm.org/en/publications/guides/gum.html>.
12. Joint Committee for Guides in Metrology, *Evaluation of Measurement Data Supplement 1 to the “Guide to the Expression of Uncertainty in Measurement Propagation of Distributions Using a Monte Carlo Method*, 1st Edition, BIPM, Sèvres-France, 2008, Available at: <http://www.bipm.org/en/publications/guides/gum.html>, <http://www.bipm.org/en/publications/guides/gum.html>.
13. Azpúrua, M. A., C. Tremola, and E. Páez, “Comparison of the gum and monte carlo methods for the uncertainty estimation in electromagnetic compatibility testing,” *Progress In Electromagnetics Research B*, Vol. 34, 125–144, 2011.

14. Koch, K. R., "Evaluation of uncertainties in measurements by Monte-Carlo simulations with an application for laserscanning," *Journal of Applied Geodesy*, Vol. 2, 67–77, 2008.
15. Jing, H., M.-F. Huang, Y.-R. Zhong, B. Kuang, and X.-Q. Jiang, "Estimation of the measurement uncertainty based on quasi monte-carlo method in optical measurement," *Proceedings of the International Society for Optical Engineering*, 2007.
16. Khu, S. T. and M. G. Werner, "Reduction of Monte-Carlo simulation runs for uncertainty estimation in hydrological modelling," *Hydrology and Earth System Sciences*, Vol. 7, No. 5, 680–690, 2003.
17. Andræ, A. S. G., P. Müller, J. Anderson, and J. Liu, "Uncertainty estimation by monte carlo simulation applied to life cycle inventory of cordless phones and microscale metallization processes," *IEEE Transactions on Electronics Packaging Manufacturing*, Vol. 27, No. 4, 233–245, 2004.
18. Schuëller, G. I., "On the treatment of uncertainties in structural mechanics and analysis," *Journal Computers and Structures*, Vol. 85, Nos. 5-6, 235–243, 2007.
19. Paez, E., C. Tremola, and M. Azpúrua, "A proposed method for quantifying uncertainty in RF immunity testing due to eut presence," *Progress In Electromagnetics Research B*, Vol. 29, 175–190, 2011.
20. Stratton, J. A., *Electromagnetic Theory*, McGraw-Hill Book Company, Inc., 1941.
21. Pozar, D. M., *Microwave Engineer*, John Wiley & Sons, 2005.
22. Willink, R., "On using the Monte Carlo method to calculate uncertainty intervals," *Metrologia*, Vol. 43, L39–L42, 2006.